

# Magnetotransport effects in polar versus non-polar SrTiO<sub>3</sub> based heterostructures

E. Flekser,<sup>1</sup> M. Ben Shalom,<sup>1</sup> M. Kim,<sup>2</sup> C. Bell,<sup>2</sup> Y. Hikita,<sup>2</sup> H. Y. Hwang,<sup>2</sup> and Y. Dagan<sup>1</sup>

<sup>1</sup>*Raymond and Beverly Sackler School of Physics and Astronomy, Tel-Aviv University, Tel Aviv, 69978, Israel*

<sup>2</sup>*Stanford Institute for Materials and Energy Sciences,*

*SLAC National Accelerator Laboratory, Menlo Park, CA 94025, USA*

(Dated: August 11, 2018)

Anisotropic magnetoresistance and negative magnetoresistance for in-plane fields are compared for the LaAlO<sub>3</sub>/SrTiO<sub>3</sub> interface and the symmetric Nb-doped SrTiO<sub>3</sub> heterostructure. Both effects are exceptionally strong in LaAlO<sub>3</sub>/SrTiO<sub>3</sub>. We analyze their temperature, magnetic field and gate voltage dependencies and find them to arise from a Rashba type spin-orbit coupling with magnetic scatterers that have two contributions to their potential: spin exchange and Coulomb interaction. Atomic spin-orbit coupling is sufficient to explain the small effects observed in Nb-doped SrTiO<sub>3</sub>. These results clarify contradicting transport interpretations in SrTiO<sub>3</sub>-based heterostructures.

PACS numbers: 75.70.Cn, 73.40.-c

The interface between oxides can exhibit electronic properties that are substantially different from those of its constituting materials[1]. The most studied example is the conducting interface formed between SrTiO<sub>3</sub> and LaAlO<sub>3</sub> [2], which exhibits superconductivity [3] with a tunable critical temperature [4]. Various probes showed evidence for magnetic effects at the interface: hysteresis in the magnetoresistance at low temperatures [5, 6], SQUID magnetometry [7] showed ferromagnetic response for samples deposited at high oxygen pressure, and recently scanning SQUID microscopy [8] and torque magnetometry [9] measurements suggested the coexistence of superconductivity and ferromagnetism. Theoretical model explaining this coexistence has been proposed [10]. It has been found that the magnetic state is not related to itinerant electrons but to localized moments that are independent of carrier concentration [11]. Magnetic moments were not observed in SrTiO<sub>3</sub>/Nb-doped SrTiO<sub>3</sub> (Nb/SrTiO<sub>3</sub>) heterostructures suggesting that magnetism is related to the polar discontinuity characterizing LaAlO<sub>3</sub>/SrTiO<sub>3</sub>, or to a strong electric field applied at the surface [12, 13]. Another view based on studies of La-doped SrTiO<sub>3</sub> system is that magnetism in SrTiO<sub>3</sub> based systems appears at high carrier concentrations[14].

While the superconducting state has a conspicuous signature in transport measurements, such a signature for the magnetic state remains illusive. M. Ben Shalom *et al.* showed that a strong magnetoresistance anisotropy is observed together with superconductivity. They interpreted their data in terms of anisotropic spin scattering resulting from magnetic ordering together with a strong spin-orbit interaction[15, 16]. This spin-orbit interaction was measured using its effect on the transport properties in the normal and in the superconducting state [17] and in the weak localization regime [18]. Furthermore, Seri and Klein suggested that the anomalous behavior of the Hall signal is a result of a field induced magnetism [19].

There are various SrTiO<sub>3</sub> based systems that exhibit

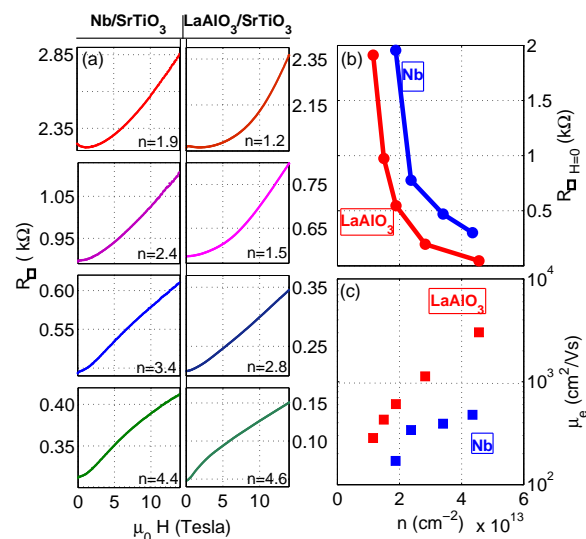


FIG. 1: Color on-line (a) Sheet resistance of LaAlO<sub>3</sub>/SrTiO<sub>3</sub> (Sample 1) and Nb/SrTiO<sub>3</sub> as a function of magnetic field for the various carrier concentrations  $n$  denoted in units of  $10^{13}$  cm<sup>-2</sup> and varied using back-gate voltage. (b) The sheet resistance at 2 K versus  $n$  for the two types of samples. (c) The mobility inferred from (b) as a function of  $n$ .

properties of a two dimensional electron gas [12, 13, 20–25]. Of these systems Nb/SrTiO<sub>3</sub> has the most symmetric structure, it also lacks polarization existing in the other systems. It is therefore worth to carefully compare the anisotropy of the transport properties of Nb/SrTiO<sub>3</sub> and LaAlO<sub>3</sub>/SrTiO<sub>3</sub>.

Superconductivity and spin-orbit interaction in Nb/SrTiO<sub>3</sub> were studied by M. Kim *et al.* [26]. They found that the upper critical field exceeds the Clogston-Chandrasekhar limit with values similar to LaAlO<sub>3</sub>/SrTiO<sub>3</sub>. They suggested that the spin-orbit interaction plays an important role also in Nb/SrTiO<sub>3</sub>, thus raising questions on a purely Rashba type spin-orbit

coupling model for the various systems.

In the study we present here, we compare the magnetoresistance and anisotropic magnetoresistance (AMR) in the two dimensional electron gas in heterostructures of Nb/SrTiO<sub>3</sub> and LaAlO<sub>3</sub>/SrTiO<sub>3</sub>. The large negative magnetoresistance observed for in-plane magnetic fields (nPMR) in LaAlO<sub>3</sub>/SrTiO<sub>3</sub> is absent in Nb/SrTiO<sub>3</sub> for the carrier densities under study. We show that the AMR observed when rotating the in-plane magnetic field with respect to the current direction and the nPMR arise from the same mechanism. From the sign and magnitude of the AMR effect we conclude that polarized magnetic scatterers and a Rashba type spin-orbit interaction are responsible for this effect. This scattering process is absent in the symmetric structure of Nb/SrTiO<sub>3</sub> where a smaller and opposite in sign effect is seen.

Thin films of LaAlO<sub>3</sub> were deposited by a pulsed laser on atomically flat SrTiO<sub>3</sub> substrates with : 6, 8 and 10 unit cells respectively. The oxygen pressure during the deposition was maintained at  $10^{-4}$  Torr and the temperature was 785 °C. The deposition was followed by a two-hour annealing stage at oxygen pressure of 0.2 Torr and a temperature of 500° C. The thickness of the LaAlO<sub>3</sub> layer was monitored by reflection high-energy electron diffraction. The samples were patterned into narrow strips or into Hall bars [27]. A Nb/SrTiO<sub>3</sub> sample with 1% Nb 6.7 nm thick with 100 nm SrTiO<sub>3</sub> buffer and capping layers was deposited as described elsewhere [28]. A layer of gold was evaporated at the bottom of the sample and used as a gate when biased to  $\pm 100$  V relative to the 2DEG. Contacts to the LaAlO<sub>3</sub>/SrTiO<sub>3</sub> samples were made by drilling holes through the LaAlO<sub>3</sub> layer using ion irradiation followed by sputtering Ti/Al or Ti/Au pads.

We have previously showed that in the presence of a large parallel magnetic field a small perpendicular component can result in a dramatic increase in resistance [16]. A small deviation from exact parallel position (e.g. due to a wobble in the rotator probe) can therefore have a strong undesired effect on the data. In order to avoid this spurious effect we simultaneously measured two perpendicular bridges on the same substrate and made sure that all reported effects are phase shifted by 90° between the two bridges. For example for current running along the [110] direction we had another bridge with current running along the  $[1\bar{1}0]$  direction.

In Fig.1a we compare the sheet resistance versus magnetic field curves for LaAlO<sub>3</sub>/SrTiO<sub>3</sub> and Nb/SrTiO<sub>3</sub> at 2 K. Here the magnetic field is applied perpendicular to the conducting plane. The carrier concentration is varied by the gate voltage and estimated from the high field slope of the Hall resistance ( $\mu_0 H > 12$  T). For LaAlO<sub>3</sub>/SrTiO<sub>3</sub> the typical dependence of longitudinal and Hall resistivity on gate and temperature is observed [29]. The dependencies of the sheet resistance and mobility as a function of carrier concentra-

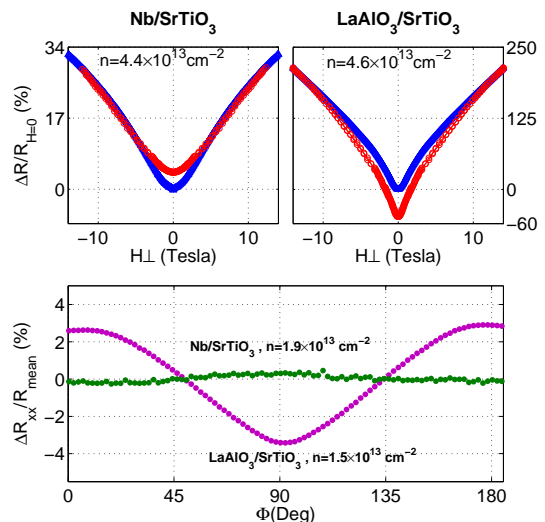


FIG. 2: (Color on-line) Upper panel: Magnetoresistance comparison between magnetic field applied perpendicular to the plane swept between -14 to 14 T (blue triangles) and rotation in a constant field of 14 T thus varying the perpendicular component (red circles) for Nb/SrTiO<sub>3</sub> and LaAlO<sub>3</sub>/SrTiO<sub>3</sub> (Sample 1) at 2 K. Negative magnetoresistance is observed only for LaAlO<sub>3</sub>/SrTiO<sub>3</sub>. Lower panel: Anisotropic magnetoresistance for in-plane field of 18 T rotated with respect to the current direction at 20 mK. Large positive AMR is observed for LaAlO<sub>3</sub>/SrTiO<sub>3</sub>. A smaller effect is observed for Nb/SrTiO<sub>3</sub> with an opposite sign.

tion are shown in Fig.1b. The first significant difference between Nb/SrTiO<sub>3</sub> and LaAlO<sub>3</sub>/SrTiO<sub>3</sub> is revealed when applying a magnetic field component parallel to the plane. In Fig.2 (upper panel) we show two data sets for each sample: triangles are data taken while sweeping the magnetic field perpendicular to the conducting plane. The circles represent data taken while holding a constant magnetic field of 14 T and changing the angle  $\theta$  between the field and the plane. The sheet resistance is plotted against the perpendicular field amplitude (component) for the field sweep (rotation) experiments. While for the LaAlO<sub>3</sub>/SrTiO<sub>3</sub> a strong pronounced negative magnetoresistance is seen when a significant parallel field component is present, such a component contributes a merely small positive magnetoresistance for the Nb/SrTiO<sub>3</sub> sample. For example,  $H_{\perp}=0$  for the circles corresponds to 14 T applied parallel to the plane resulting in a positive magnetoresistance for the Nb/SrTiO<sub>3</sub> and a strong negative magnetoresistance for LaAlO<sub>3</sub>/SrTiO<sub>3</sub>. The small in-plane positive magnetoresistance in Nb/SrTiO<sub>3</sub> is a result of the 90° angle between the in-plane field and the current. The absence of nPMR in Nb/SrTiO<sub>3</sub> holds for all carrier concentrations studied here and is one of the key findings reported in this Letter.

Rotating the in-plane magnetic field with respect to

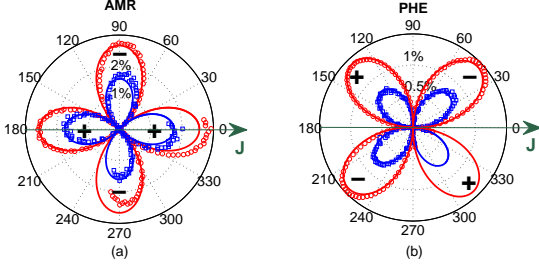


FIG. 3: Color on-line (a) The anisotropic magnetoresistance normalized to its mean value (Sample 1),  $\frac{\Delta R_{xx}}{R_{\text{mean}}}$  as a function of  $\phi$  the angle between the current and the magnetic field (18 T) at 20 mK in polar representation. Data are presented for two carrier concentrations (controlled by the gate voltage) circles  $n = 1.8 \times 10^{13} \text{ cm}^{-2}$  blue squares  $n = 1.3 \times 10^{13} \text{ cm}^{-2}$  the solid lines are fits to  $\cos^2(\phi)$  (b) The transverse voltage signal normalized to the mean longitudinal voltage ( $V_{xx}$ ) in (a). This planar Hall signal is shifted by  $45^\circ$  relative to the longitudinal signal as expected. Solid lines are fits to  $\cos^2(\phi - \frac{\pi}{4})$ .

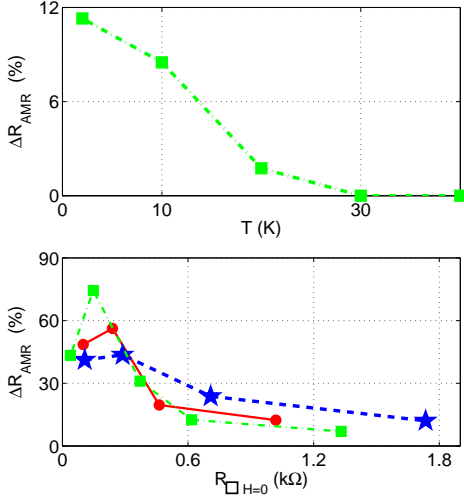


FIG. 4: Color on-line. Upper panel AMR amplitude:  $\Delta R_{AMR} = \frac{\rho_{||} - \rho_{\perp}}{(\rho_{||} + \rho_{\perp})/2}$  as a function of temperature. Lower panel: AMR amplitude as a function of the zero field resistance controlled by gate voltage for various samples: Green squares (Sample 1) are data taken at 20 mK and 18 T for current along [100]. Red circles (Sample 2) and blue stars (Sample 3) are data taken at 2 K and 14 T for bridges along [110] (red) and [100] (blue). (see also supplementary part).

the current unravels another important difference between Nb/SrTiO<sub>3</sub> and LaAlO<sub>3</sub>/SrTiO<sub>3</sub>. The AMR amplitude,  $\Delta R_{AMR} = \frac{\rho_{||} - \rho_{\perp}}{(\rho_{||} + \rho_{\perp})/2}$ , is large and positive for LaAlO<sub>3</sub>/SrTiO<sub>3</sub> (i.e. maximum resistance for  $\vec{H} \parallel \vec{J}$  and minimum for  $\vec{H} \perp \vec{J}$  with  $\vec{J}$  being the current density). By contrast, for Nb/SrTiO<sub>3</sub> it is very small and negative.

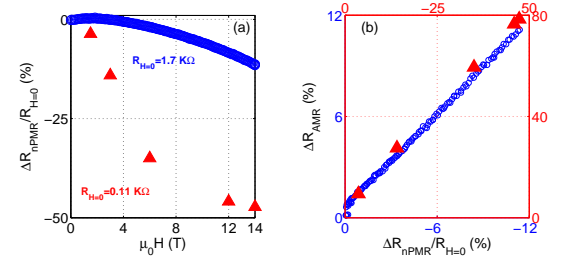


FIG. 5: Color on-line (a) nPMR effect  $\frac{\Delta R_{xx}(H_{||})}{R_0}$  as a function of magnetic field (Sample 3) for two gate voltages at 2 K. (b) AMR versus the nPMR for the same gate voltages. We note that the two effects scale.

Anisotropy in the longitudinal conductivity (such as the AMR) should result in a planar Hall signal. In this configuration the transverse voltage signal is measured for in-plane fields as a function of the angle between the field and current. This signal should be phase shifted by  $45^\circ$  compared to the longitudinal AMR [30].

In Fig.3a we show the AMR for two gate voltages in polar representation. Note that the angular dependence follows  $\cos^2 \phi$  with  $\phi$  the angle between the current and the field. The corresponding planar Hall effect (PHE) is shown in Fig.3b. The fact that the AMR and PHE signal are observed with the proper phase shift of  $45^\circ$  and with an amplitude ratio of 1/2 ensures that the anisotropy is an intrinsic property, unrelated to a spurious measurement artifact.

In Fig.4a we study the temperature dependence of the AMR. The AMR disappears at  $\sim 30$  K for all gate voltages. This is the temperature above which the nPMR disappears, consistent with our previous observations [16]. The fact that both AMR and the nPMR vanish at the same temperature suggests that they are two expressions of the same scattering mechanism.

The amplitude of the AMR is shown versus the sheet resistance in Fig.4b. for three different samples in the maximal accessible field. Here we use the sheet resistance as a useful parameter (monotonic with carrier concentration) for comparison of different samples. We note that no significant difference in the AMR amplitude is observed when the current direction is along [110] or [100] (See supplementary information for more details). This suggests that the most important parameter affecting the AMR is the angle between the current and field. We emphasize that standard defects cannot result in such strong variation in AMR amplitude with gate: from a few percent at low carrier concentration to 85%.

The final evidence that the nPMR and AMR originate from the same scattering mechanism is found from their field dependence as demonstrated in Fig.5. We show two data sets of high and low carrier concentrations for the same sample. The nPMR exhibits very different field

dependence (Left hand panel) for these two concentrations. Furthermore, for the high carrier concentration the field dependence of the nPMR has a few characteristic features: starting with a flat region followed by a steep descent and a saturation regime [17]. Nevertheless, the amplitude of the AMR tracks this behavior. The two effects have similar field dependence up to a numerical coefficient. This is clear from Fig.5b. where we plot the amplitude of the AMR versus the nPMR for the above gate voltages. Indeed a linear dependence is obtained.

Since both nPMR and AMR effects exhibit the same temperature and magnetic field dependencies for various carrier concentrations they must arise from the same scattering mechanism. This key observation allows us to focus on the mechanism responsible for the AMR and thus the other magnetotransport effects.

Three possible mechanisms for the AMR have been proposed [31]: a. anisotropic Fermi velocities coupled to a finite magnetization through the spin-orbit interaction, b. spin-orbit coupled magnetically polarized carriers with isotropic scattering centers, and c. anisotropic magnetic scattering centers acting on unpolarized spin-orbit coupled carriers. Mechanisms a. and b. usually result in a smaller AMR effect since the magnetization and the spin-orbit interaction compete with each other. This is not the case in mechanism c. where the magnetization and the spin orbit interaction do not exist in the same band states, thus allowing fully polarized scatterers despite the strong spin-orbit interaction. The unusually large AMR (up to 85%) suggests that the dominant mechanism in  $\text{LaAlO}_3/\text{SrTiO}_3$  is mechanism c.

The nature of the scattering centers in mechanism c. can be either purely magnetic (only spin exchange) or electro-magnetic (combined with the Coulomb interaction). Large AMR can be observed only if the Fermi energy,  $E_F$  is much smaller than the spin-orbit interaction for the first case. Calculations for the case of electro-magnetic scatterers show that the AMR amplitude can be very large (twice as large as for the pure magnetic case) even for a spin-orbit interaction smaller than  $E_F$ . In this case the amplitude of the AMR strongly depends on the ratio between the electric and the magnetic parts of the scattering potential, with a sharp maximum at the point where this ratio becomes unity. The origin of this large AMR is a destructive interference between the magnetic and the non-magnetic back-scattering amplitudes [32].

As can be seen in Fig.4b the AMR is large for a broad range of concentrations and sheet resistances. Since in  $\text{LaAlO}_3/\text{SrTiO}_3$  the spin-orbit interaction is of the order of  $E_F$ , the scattering potential should include an electric part. This suggests that localized charges act as both electric and magnetic scattering centers and the maximum AMR should not necessarily coincide with the maximum of spin-orbit interaction. Upon changing the gate voltage we identify the maximum in AMR as the point where the magnetic and electric scattering amplitude ra-

tio becomes of the order one. Moving away from this point will alter this ratio by either screening the electric scattering or by moving the wave function away from the interface and consequently reduce the coupling between the magnetic scatterers and the conduction electrons.

A more detailed description of our system should include the way the spin-orbit interaction changes with carrier concentration. In addition, as the carrier density increases the  $d_{yz}$  and  $d_{xz}$  bands become populated and the anisotropy of the band mass may become important [33].

Spin-orbit interaction at the atomic level without coupling the band momentum to the spin is not expected to result in AMR. Large AMR amplitude is expected if the Rashba or the Dresselhaus effects take place. However, the sign of the AMR is positive, i.e. maximum resistance for magnetic field parallel to the current for the Rashba and negative for the Dresselhaus one [32]. This allows us to conclude that the main contribution to the AMR in  $\text{LaAlO}_3/\text{SrTiO}_3$  comes from the Rashba effect.

For  $\text{Nb}/\text{SrTiO}_3$  large spin-orbit coupling has been suggested based on the large  $H_{c2}$  parallel magnetic field needed to quench superconductivity [26]. However, in this case the AMR is very small and negative. We therefore explain the large  $H_{c2}$  observed by M. Kim *et al.* as a result of atomic spin-orbit interaction[34]. The small negative AMR can be a result of a finite thickness of the confinement zone [16]. For  $\text{Nb}/\text{SrTiO}_3$  at the carrier concentration studied, both magnetism and the Rashba term do not play a significant role in transport.

A negative contribution to the AMR can be seen in  $\text{LaAlO}_3/\text{SrTiO}_3$  at low temperatures for large carrier concentrations.[16] In these concentrations the AMR deviates from the simple  $\cos^2(\phi)$  and becomes sharp. This effect is seen both for current running along [100] and [110] directions. It is therefore less likely to be related to a crystalline magnetic anisotropy.

In summary, we show that anisotropic magnetoresistance (AMR) and planar Hall effect are observed in  $\text{LaAlO}_3/\text{SrTiO}_3$  when rotating the magnetic field in-plane with respect to the current. We show that the AMR scales with the in-plane negative magnetoresistance (nPMR). This suggests that both effects arise from the same spin scattering mechanism combined with a strong spin-orbit interaction. Importantly, the AMR is very small and negative and the nPMR is absent in the non-polar symmetric structure of Nb-doped  $\text{SrTiO}_3$  for the carrier range under study. Since the AMR has similar amplitudes for current flowing along different crystallographic directions:  $\vec{J}||[110]$  or  $\vec{J}||[100]$ , the important parameter governing it is the angle between field and current. The sign of the effect in  $\text{LaAlO}_3/\text{SrTiO}_3$  shows that the spin-orbit interaction involved in the scattering process is of the Rashba type. This is not the case in  $\text{Nb}/\text{SrTiO}_3$  where atomic spin-orbit interaction is sufficient to explain the small effects observed. The large magnitude of the AMR effect in the polar structure is ex-

plained by a scattering potential with two components: spin exchange and Coulomb interaction. The ratio between these contributions varies with gate voltage, which results in a strong gate dependence. The fact that mobile carriers and the magnetic moments do not occupy the same band state may allow coexistence of superconductivity and magnetism.

We thank K. Michaeli, K. Vyborny, S. Ilani and I. Neder for useful discussions. This research was partially supported by Grant No. 2010140 from the United States-Israel Binational Science Foundation; by the Infrastructure program of the Israeli Ministry of Science and Technology and by the Israel Science Foundation under grant 1421/08. M.K., C.B. Y.H. and H.Y.H. acknowledge support by the Department of Energy, Office of Basic Energy Sciences, Materials Sciences and Engineering Division, under contract DE-AC02-76SF00515. A portion of this work was performed at the National High Magnetic Field Laboratory, which is supported by NSF Cooperative Agreement No. DMR-0654118, by the State of Florida, and by the DOE.

- 
- [1] S. Okamoto and A. J. Millis, *Nature (London)* **428**, 630 (2004).
  - [2] A. Ohtomo and H. Y. Hwang, *Nature (London)* **427**, 423 (2004).
  - [3] N. Reyren, S. Thiel, A. Caviglia, L. Kourkoutis, G. Hammerl, C. Richter, C. Schneider, T. Kopp, A. Rüetschi, D. Jaccard, et al., *Science* **317**, 1196 (2007).
  - [4] A. Caviglia, S. Gariglio, N. Reyren, D. Jaccard, T. Schneider, M. Gabay, S. Thiel, G. Hammerl, J. Mannhart, and J. Triscone, *Nature* **456**, 624 (2008).
  - [5] A. Brinkman, M. Huijben, M. Van Zalk, J. Huijben, U. Zeitler, J. Maan, W. Van der Wiel, G. Rijnders, D. Blank, and H. Hilgenkamp, *Nature Materials* **6**, 493 (2007).
  - [6] D. A. Dikin, M. Mehta, C. W. Bark, C. M. Folkman, C. B. Eom, and V. Chandrasekhar, *Phys. Rev. Lett.* **107**, 056802 (2011).
  - [7] X. Wang, G. Baskaran, Z. Liu, J. Huijben, J. Yi, A. Anadi, A. Barman, A. Rusydi, S. Dhar, Y. Feng, et al., *Nature Communications* **2**, 188 (2011).
  - [8] J. A. Bert, B. Kalisky, C. Bell, M. Kim, Y. Hikita, H. Y. Hwang, and K. A. Moler, *Nature Physics* **7**, 767 (2011).
  - [9] L. Li, C. Richter, J. Mannhart, and R. Ashoori, *Nature Physics* **7**, 762 (2011).
  - [10] K. Michaeli, A. Potter, and P. Lee, *Physical Review Letters* **108**, 117003 (2012).
  - [11] B. Kalisky, J. A. Bert, B. B. Klopfer, C. Bell, H. K. Sato, M. Hosoda, Y. Hikita, H. Y. Hwang, and K. A. Moler, *Nat. Commun.* **3**, 922 (2012).
  - [12] Y. Lee, C. Clement, J. Hellerstedt, J. Kinney, L. Kinischtzke, X. Leng, S. D. Snyder, and A. M. Goldman, *Physical Review Letters* **106**, 136809 (2011).
  - [13] M. Lee, J. Williams, S. Zhang, C. Frisbie, and D. Goldhaber-Gordon, *Physical Review Letters* **107**, 256601 (2011).
  - [14] P. Moetakef, J. R. Williams, D. G. Ouellette, A. Kajdos, D. Goldhaber-Gordon, S. J. Allen, and S. Stemmer, *Physical Review X* **2**, 021014 (2012).
  - [15] M. Sachs, D. Rakhmievitch, M. B. Shalom, S. Shefler, A. Palevski, and Y. Dagan, *Physica C: Superconductivity* **470**, S746 (2010).
  - [16] M. Ben Shalom, C. Tai, Y. Lereah, M. Sachs, E. Levy, D. Rakhmievitch, A. Palevski, and Y. Dagan, *Physical Review B* **80**, 140403 (2009).
  - [17] M. Ben Shalom, M. Sachs, D. Rakhmievitch, A. Palevski, and Y. Dagan, *Physical Review Letters* **104**, 126802 (2010).
  - [18] A. D. Caviglia, M. Gabay, S. Gariglio, N. Reyren, C. Cancellieri, and J. Triscone, *Physical Review Letters* **104**, 126803 (2010).
  - [19] S. Seri and L. Klein, *Phys. Rev. B* **80**, 180410 (2009).
  - [20] A. Santander-Syro, O. Copie, T. Kondo, F. Fortuna, S. Pailhes, R. Weht, X. Qiu, F. Bertran, A. Nicolaou, A. Taleb-Ibrahimi, et al., *Nature* **469**, 189 (2011).
  - [21] W. Meevasana, P. King, R. He, S. Mo, M. Hashimoto, A. Tamai, P. Songsiririthigul, F. Baumberger, and Z. X. Shen, *Nature Materials* **10**, 114 (2011).
  - [22] Y. Xie, C. Bell, Y. Hikita, and H. Y. Hwang, *Adv. Mater.* **23**, 1744 (2012).
  - [23] J. Ngai, Y. Segal, D. Su, Y. Zhu, F. Walker, S. Ismail-Beigi, K. Le Hur, and C. Ahn, *Physical Review B* **81**, 241307 (2010).
  - [24] J. Biscaras, N. Bergeal, A. Kushwaha, T. Wolf, A. Rastogi, R. Budhani, and J. Lesueur, *Nature Communications* **1**, 89 (2010).
  - [25] J. Ye, S. Inoue, K. Kobayashi, Y. Kasahara, H. T. Yuan, H. Shimotani, and Y. Iwasa, *Nature materials* **9**, 125 (2009).
  - [26] M. Kim, Y. Kozuka, C. Bell, Y. Hikita, and H. Y. Hwang, *Arxiv preprint arXiv:1106.5193* (2011).
  - [27] C. W. Schneider, S. Thiel, G. Hammerl, C. Richter, and J. Mannhart, *Applied Physics Letters* **89**, 122101 (2006).
  - [28] Y. Kozuka, M. Kim, C. Bell, B. Kim, Y. Hikita, and H. Y. Hwang, *Nature* **462**, 487 (2009).
  - [29] C. Bell, S. Harashima, Y. Kozuka, M. Kim, B. G. Kim, Y. Hikita, and H. Y. Hwang, *Physical Review Letters* **103**, 226802 (2009).
  - [30] H. Tang, R. Kawakami, D. Awschalom, and M. Roukes, *Physical Review Letters* **90**, 107201 (2003).
  - [31] K. Výborný, J. Kučera, J. Sinova, A. W. Rushforth, B. L. Gallagher, and T. Jungwirth, *Phys. Rev. B* **80**, 165204 (2009).
  - [32] M. Trushin, K. Výborný, P. Moraczewski, A. A. Kovalev, J. Schliemann, and T. Jungwirth, *Phys. Rev. B* **80**, 134405 (2009).
  - [33] A. Joshua, S. Pecker, J. Ruhman, E. Altman, and S. Ilani, *Arxiv preprint arXiv:1110.2184* (2011).
  - [34] R. A. Klemm, A. Luther, and M. R. Beasley, *Phys. Rev. B* **12**, 877 (1975).